Mechanics of Advanced Composite Structures 11 (2024) 177 – 190

Semnan University

Mechanics of Advanced Composite Structures

journal homepage: https://MACS.journals.semnan.ac.ir

A Comprehensive Comparison between Multi-Objective Optimization Methods for Composite Hexagonal-Triangle Grid Structure using FSDT under External Hydrostatic Pressure

M. Soheil Shamaee *

Department of Computer Science, Faculty of Mathematical Sciences, University of Kashan, Kashan, 87317-53153, I. R. Iran.

KEYWORDS

Grid stiffeners;
Buckling load;
Composite shell;
Multi-objective optimization;
NSGAII;
MOPSO.

ABSTRACT

This study focuses on investigating how grid-stiffened composite shells behave under external hydrostatic pressure. The critical buckling load is calculated using the first-order shear deformation theory (FSDT) and the Ritz method. Various factors, including shell thickness, angle of helical stiffeners, rib section area, and the number of stiffeners, are examined to understand their impact on the buckling load. To optimize the design, three multi-objective optimization algorithms are employed: Nondominated Sorting Genetic Algorithm II (NSGAII), Multiobjective Particle Swarm Optimization (MOPSO), and a hybrid method that combines NSGAII and MOPSO. The hybrid method intelligently divides the population into two groups and uses NSGAII and MOPSO to efficiently explore and exploit the solution space. The results yield a Pareto optimal front that showcases diverse solutions across different regions, providing decision-makers with the flexibility to select the solution that best fits their preferences. The solutions obtained through these algorithms are compared based on their diversity and distribution throughout the Pareto front.

1. Introduction

A composite grid structure is a structure of composite one-directional tapes that are joined together to form a continuous set as two-dimensional (planar) or three-dimensional (spatial). Composite grid structures are more capable than metal structures due to strength, low weight, flexibility in design, easy construction, and the ability to withstand various environmental conditions. Shells that have been stiffened with grid structures are an appropriate alternative for composite, sandwich, or filled metal panels. The main objective of using grid structures is the optimization of longitudinal properties of composite materials in structures. Grid structures are being used as a new technology in many industries, especially the aerospace industry. However, in the past, several valuables of research have been conducted on this kind of structure.

Particle Swarm Optimization (PSO) [1] is a population-based optimization algorithm inspired by the social behavior of bird flocks or fish schools. It searches for the optimal solution by iteratively updating a group of candidate solutions called particles. In multi-objective problems, we have multiple conflicting objectives that we want to optimize simultaneously. Multiobjective Particle Swarm Optimization (MOPSO) [2] extends the basic PSO algorithm to handle these kinds of problems. Instead of just one solution per particle, each particle in MOPSO maintains a solution archive that stores a set of non-dominated (i.e., Pareto optimal) solutions found so far. The goal is to find diverse solutions along the Pareto front, where no solution is better than another in every objective.

The Non-Dominated Sorting Genetic Algorithm II (NSGAII) [3] is another popular evolutionary algorithm designed for multi-objective optimization problems. Like MOPSO, NSGAII also aims to find a set of non-dominated solutions. NSGAII works by maintaining a population of candidate solutions called

* Corresponding author. Tel.: +98-31-55913048; Fax: +98-31-55912501.
E-mail address: soheilshamaee@kashanu.ac.ir

DOI: 10.22075/macs.2023.31305.1540
Received 2023-07-20; Received in revised form 2023-08-16; Accepted 2023-09-07.

individuals. It uses genetic operators such as selection, crossover, and mutation to generate new offspring individuals. The algorithm then applies a non-dominated sorting procedure to sort the population into different fronts based on their dominance relationships. This helps in identifying the Pareto front solutions. By iterating and improving the population over generations, NSGAII gradually converges into a diverse and well-distributed set of non-dominated solutions. These solutions are spread across different regions of the Pareto front, which allows decision-makers to choose the solution that best suits their preferences.

Both MOPSO and NSGAII are powerful algorithms for solving multi-objective optimization problems, and they have their unique strengths and weaknesses. They have been widely applied in various fields, such as engineering, finance, and data mining, where decision-makers need to consider multiple conflicting objectives. In this paper, a hybrid algorithm which is the synergistic combination of NSGAII and MOPSO [4] is employed to find the optimal structure of grid-stiffened composite shells. This hybrid model exhibits substantial potential in terms of information exchange, parallel processing, enhanced searching capabilities, and the ability to generate more favorable results when compared to individual computational multi-objective models [4].

The exploitation and exploration processes in NSGAII and MOPSO algorithms differ. While NSGAII incorporates crossover, mutation, elitism, fast nondominated sorting, and crowding distance calculations to improve solution spread and preserve diversity, these factors can restrict the convergence of NSGAII. On the other hand, MOPSO particles operate without genetic operators, utilizing a unique information-sharing mechanism distinct from NSGAII. They explore the solution space by updating velocity and inertia weight, with guidance from a leader selected from the Pareto optimal solutions stored in an external memory called the repository. However, the MOPSO algorithm can encounter challenges in complex problems, often getting trapped in local optima.

To prevent the capture of global solutions in local optima, a hybrid multi-objective algorithm must strike a balance between exploitation and exploration. The hybrid model aims to enhance the overall search mechanism by combining NSGAII and MOPSO, which employ distinct approaches to explore and exploit the search space. In this algorithm, the exploration phase is performed by NSGAII, utilizing the top half of the population. NSGAII thoroughly explores every region of the solution space to obtain a comprehensive evaluation of global solutions. On the other hand, MOPSO is responsible for the exploitation task, employing the lower half of the population. By integrating these two complementary algorithms, the hybrid model effectively combines their strengths in exploring and exploiting the search space, resulting in an improved overall search mechanism.

The study focuses on examining a grid structure consisting of hexagonal-triangle stiffeners within a stiffened composite cylindrical shell. By utilizing the smeared method and employing linear FSDT (First-order Shear Deformation Theory), the critical buckling pressure of the structure can be determined. Recognizing the industry's emphasis on lightweight structures, the study also includes an optimization process for the grid structures to reduce weight while maximizing the critical buckling load. Three multi-objective optimization meta-heuristic algorithms, namely NSGAII, MOPSO, and a hybrid method combining NSGAII and MOPSO, are applied. The outcomes of these methods generate Pareto fronts, which offer a range of solutions across different regions. This enables decision-makers to select the solution that best matches their specific preferences and requirements.

The remaining sections of the paper are structured as follows. Section 2 provides a concise summary of the relevant previous studies. Sections 3 and 4 present the equations, assumptions, and the equivalent representation of composite grid shells. Section 5 outlines the optimization process for grid shells using our proposed multi-objective meta-heuristic methods, followed by the presentation of numerical results. Finally, Section 6 concludes the paper.

2. Related Works

In this section, we provide a concise overview of the studies that are relevant to our topic. Genetic algorithms (GAs) are a type of evolutionary method that is well-suited for addressing optimization problems. Several studies have shown that GAs perform effectively in finding close-to-optimal solutions for discrete optimization problems, including composite structures [5-8].

Kim [9] conducted research on constructing composite grid cylinders, focusing on the analysis of their building process, buckling strength, and the effects of a vertical compressive force. The study explored the impact of this force on buckling, rib failure, and the overall stability of the structure. In [9], the author's focus shifted to grid composite panels rather than grid cylinders. Their investigation involved analyzing various aspects such as buckling modes, rib failure, shell

performance, and the overall failure behavior of the entire structure.

The researchers in [10] conducted a study on optimizing a rotating structure featuring variable curvature. This structure consisted of a shell and a composite grid structure. The primary objective of the optimization problem was to minimize the weight of the structure. By adjusting the size and rib spacing, the aim was to achieve the lowest possible weight while ensuring that the structure maintained sufficient strength to resist local buckling.

Following that, Zhang and colleagues [11] published an article introducing two novel grid structures and conducted a comprehensive analysis of their mechanical properties. These structures were formed by combining existing known structures. Furthermore, the authors verified the derived properties of these structures using the finite element method, ensuring their accuracy and reliability.

In their experimental research, Yazdani and colleagues [12] investigated the buckling behavior of composite grid shells under axial load. Through their study, they deduced that increasing the number of helical ribs had a more significant impact compared to adding circumferential rings or altering the grid type. Additionally, they found that shells featuring diamond-shaped grids exhibited superior performance when subjected to axial loading.

Jingxuan and colleagues [13] conducted an experiment involving the application of axial load on an advanced grid-stiffened (AGS) composite structure. They focused on assessing the structural strength and determining the failure threshold of the investigated AGS composite. To validate their findings, the results were compared with those obtained through finite element analysis using ANSYS commercial software. In reference [14], an explanation was provided regarding grid composite structures, their construction methodology, as well as the latest advancements, and their applications in the space industry. The research highlighted the role of ribs within the grid structure, which effectively enhanced the structural integrity and concurrently reduced its overall weight.

Weber and Middendorf [15] incorporated the interaction between neighboring skin areas when determining the local skin buckling load. They achieved this by implementing periodic boundary conditions at the opposite edges of the panel. Additionally, they took into account the self-stiffening impact of grid-stiffened structures resulting from the interaction with adjacent skin areas. This led to a substantial improvement in the buckling resistance of these structures.

Liu and Paavola [16] conducted a comprehensive assessment of a universal analytical sensitivity analysis approach for composite laminated panels and shells. This approach was employed for both classical laminate plate theory (CLPT) and first-order shear deformation theory (FSDT) using finite element methods as the basis.

Deveci [17] utilized a hybrid algorithm to optimize the buckling behavior of composite laminates while adhering to the Puck failure criterion constraint. Their study introduced an optimization approach aimed at identifying the optimal stacking sequence designs of laminated composite plates within various fiber angle ranges to achieve maximum resistance against buckling.

Ghasemi et al. [18] introduced an enhanced version of the NSGA-II evolutionary algorithm for the multi-objective optimization of a composite cylindrical shell subjected to external hydrostatic pressure. The study considered mass, cost, and buckling pressure as fitness functions while taking into account failure criteria as optimization objectives. Design variables such as material type, number of layers, and fiber orientations were also considered in the optimization process.

Hajmohammad et al. [19] devised a practical analytical method to determine the optimal fiber orientation for the design of fiber-reinforced polymer pressure vessels (FRPPVs) exposed to hydrostatic pressure. They employed a genetic algorithm (GA) to obtain the ideal orientation pattern that minimizes weight and maximizes buckling load.

Ghasemi et al. [20] introduced a multi-step optimization technique for predicting the optimal fiber orientation in glass fiber-reinforced polymer (GFRP) composite shells. Their method combines a refined genetic algorithm (GA) with an analytical approach to evaluate the failure behavior of the tubular structure.

Soltani et al. [21] examined the lateral buckling analysis and layup optimization of tapered thin-walled I-beams with laminated composite web and flanges. Their study aimed to maximize the lateral-torsional stability strength while minimizing the overall mass of the structure. The fitness function incorporated critical factors such as lateral buckling strength and structural mass while considering constraints such as ply angle, number of layers for the web and flanges, and section wall thickness. To achieve optimization, NSGA-II was utilized in combination with a well-defined objective function.

Hosseini et al. [22] conducted a study on the natural frequency analysis of a partially submerged FG composite rectangular plate. The investigation focused on analyzing the plate's

vibrational characteristics when in contact with a bounded fluid medium.

Arshid et al. [23] examined the thermal buckling, bending, and free vibration behavior of a porous nanocomposite annular plate at a micro-scale. The study specifically investigated the plate's response to thermal effects, taking into account the reinforcement of the plate with functionally graded GNPs (graphene nanoplatelets).

Soheil Shamaee et al. [24] analyzed the critical buckling pressure and optimal parameters for stiffeners under external hydrostatic pressure. They also optimized the stiffener parameters through a genetic algorithm (GA), resulting in a structure with minimum mass and increased buckling load compared to non-stiffened structures.

3. Equations and Assumptions

In this study, we consider a cylindrical shell stiffened by grid stiffeners which have length L, thickness t, and diameter D. Equations and assumptions about this shell are similar to those in [24]. Therefore, we won't mention those details here, but you can refer to [24] for more information.

The equations below describe the displacements in cylindrical coordinates based on the first-order shear deformation theory (FSDT). The variables u, v, and w represent the displacement components at any point on the shell, while u_0,v_0, and w_0 represent the displacement components at the middle level. Additionally, ψ_x and ψ_θ are denote the rotation from the x-axis and θ, respectively [25].

$$u(x,\theta,z) = u_0(x,\theta) + z\psi_x(x,\theta) \quad (1)$$

$$v(x,\theta,z) = v_0(x,\theta) + z\psi_\theta(x,\theta) \quad (2)$$

$$w(x,\theta,z) = w_0(x,\theta) \quad (3)$$

4. Making Equivalent of Composite Grid Shells

Jaunky et al. [26] introduced a smeared method for evaluating interactions between the shell and the stiffener, while Kidane et al. [27] presented a method to study the axial buckling of the grid composite cylinder using the same theory. The method involves calculating strains and forces in the stiffeners to create an equivalent representation. By determining a shell with the appropriate thickness that matches the stiffness of the stiffeners, the individual stiffeners are replaced, and the combined structure is treated as a unified unit.

4.1. Force Analysis in the Stiffeners

$$\begin{cases} \varepsilon_{xx} = \varepsilon_{xx}^{(0)} + (\frac{t}{2})k_{xx} \\ \varepsilon_{\theta\theta} = \varepsilon_{\theta\theta}^{(0)} + (\frac{t}{2})k_{\theta\theta} \\ \gamma_{x\theta} = \gamma_{x\theta}^{(0)} + (\frac{t}{2})k_{x\theta} \end{cases} \quad (4)$$

$$\begin{cases} \gamma_{xz} = \gamma_{xz}^{(0)} \\ \gamma_{\theta z} = \gamma_{\theta z}^{(0)} \end{cases} \quad (5)$$

When the entire structure is loaded, the reaction forces in the stiffeners are transformed into axial forces in the stiffener section (represented as F_l.). However, during this loading, the stiffeners also experience shear loads and planar shear loads, denoted as F_{lt} and F_{lz}, respectively. By solving the strains along and perpendicular to the stiffeners, the forces in the stiffeners are determined based on the strains.

$$F_{l1} = A_{st}E_l\varepsilon_{l1} = A_{st}E_l(c^2\varepsilon_{xx} + s^2\varepsilon_{\theta\theta} - cs\gamma_{x\theta}) \quad (6)$$

$$F_{l2} = A_{st}E_l\varepsilon_{l2} = A_{st}E_l(c^2\varepsilon_{xx} + s^2\varepsilon_{\theta\theta} + cs\gamma_{x\theta}) \quad (7)$$

$$F_{l2} = A_{st}E_l\varepsilon_{l3} = A_{st}E_l(\varepsilon_{\theta\theta}) \quad (8)$$

4.2. Moment Analysis of the Stiffener

The moments exerted on the stiffeners at the interface connecting the shell and stiffener result from the presence of shear forces. Utilizing the method outlined in the preceding section, we can determine the applied moment on the edges of the unit cell by referring to equations (9), (10), and (11).

Components of shear strains ε_{lz} can be obtained by considering a plane with a normal vector Z:

$$M_x = \left(\frac{2A_{st}E_lc^3}{a}\varepsilon_{xx} + \frac{2A_{st}E_lcs^2}{a}\varepsilon_{\theta\theta} + \frac{2A_{st}G_{lt}sc^2}{a}\gamma_{x\theta} - \frac{2A_{st}G_{lt}s^3}{a}\gamma_{x\theta}\right)\left(\frac{t+h}{2}\right) \quad (9)$$

$$M_\theta = \left(\frac{2A_{st}E_lsc^2}{b}\varepsilon_{xx} + \frac{2A_{st}E_l(s^3+1)}{b}\varepsilon_{\theta\theta} - \frac{2A_{st}G_{lt}c^3}{b}\gamma_{x\theta} + \frac{2A_{st}G_{lt}cs^2}{b}\gamma_{x\theta}\right)\left(\frac{t+h}{2}\right) \quad (10)$$

$$M_{x\theta} = \left(-\frac{4A_{st}G_{lt}cs^2}{b}\varepsilon_{xx} + \frac{4A_{st}G_{lt}cs^2}{b}\varepsilon_{\theta\theta} + \frac{2A_{st}E_lsc^2}{b}\gamma_{x\theta}\right)\left(\frac{t+h}{2}\right) \quad (11)$$

$$\varepsilon_{lz} = (s\gamma_{\theta_z} + c\gamma_{xz}) \quad (12)$$

The shear forces resulting from the shear strains are determined using the following approach:

$$F_{lz1} = A_{st}G_{lz}\gamma_{lz1} = A_{st}G_{lz}(-s\gamma_{\theta_z} + c\gamma_{xz}) \quad (13)$$

$$F_{lz2} = A_{st}G_{lz}\gamma_{lz2} = A_{st}G_{lz}(s\gamma_{\theta_z} + c\gamma_{xz}) \quad (14)$$

$$F_{lz3} = A_{st}G_{lz}\gamma_{lz3} = A_{st}G_{lz}(\gamma_{\theta_z}) \quad (15)$$

By examining the forces, moments, and shear forces acting on the unit cell and then performing matrix multiplication, we can derive the stiffness matrix, as represented in equation (16). Since the shell under consideration is a laminated composite, the stiffness matrix for the shell can be expressed as equation (17) [28-29].

It is worth noting that the axial stiffness A_{ij}, coupled stiffness (bending - axial) B_{ij}, bending stiffness D_{ij}, and shear stiffness H_{ij} can be determined using equations (18), (19), (20), and (21). In these equations, K_0 represents the shear correction factor, which is typically assigned a value of 5/6 [25]. Ultimately, the composite grid shell's equivalent stiffness matrix is obtained by summing the stiffness matrix of the shell and the stiffness matrix of the stiffeners, as demonstrated in equation (22).

$$\begin{bmatrix} N_x \\ N_\theta \\ N_{x\theta} \\ M_x \\ M_\theta \\ M_{x\theta} \\ Q_x \\ Q_\theta \end{bmatrix} = \begin{bmatrix} A_{11}^{st} & A_{12}^{st} & A_{13}^{st} & B_{11}^{st} & B_{12}^{st} & B_{13}^{st} & 0 & 0 \\ A_{21}^{st} & A_{22}^{st} & A_{23}^{st} & B_{21}^{st} & B_{22}^{st} & B_{23}^{st} & 0 & 0 \\ A_{31}^{st} & A_{32}^{st} & A_{33}^{st} & B_{31}^{st} & B_{32}^{st} & B_{33}^{st} & 0 & 0 \\ B_{11}^{st} & B_{12}^{st} & B_{13}^{st} & D_{11}^{st} & D_{12}^{st} & D_{13}^{st} & 0 & 0 \\ B_{21}^{st} & B_{22}^{st} & B_{23}^{st} & D_{21}^{st} & D_{22}^{st} & D_{23}^{st} & 0 & 0 \\ B_{31}^{st} & B_{32}^{st} & B_{33}^{st} & D_{31}^{st} & D_{32}^{st} & D_{33}^{st} & 0 & 0 \\ 0 & 0 & 0 & 0 & 0 & 0 & H_{44}^{st} & H_{45}^{st} \\ 0 & 0 & 0 & 0 & 0 & 0 & H_{44}^{st} & H_{45}^{st} \end{bmatrix} \begin{bmatrix} \varepsilon_{xx}^{(0)} \\ \varepsilon_{\theta\theta}^{(0)} \\ \varepsilon_{x\theta}^{(0)} \\ k_{xx} \\ k_{\theta\theta} \\ k_{x\theta} \\ \gamma_{xz}^{(0)} \\ \gamma_{\theta z}^{(0)} \end{bmatrix} \quad (16)$$

$$S_{sh} = \begin{bmatrix} A_{11} & A_{12} & A_{13} & B_{11} & B_{12} & B_{13} & 0 & 0 \\ A_{21} & A_{22} & A_{23} & B_{21} & B_{22} & B_{23} & 0 & 0 \\ A_{31} & A_{32} & A_{33} & B_{31} & B_{32} & B_{33} & 0 & 0 \\ B_{11} & B_{12} & B_{13} & D_{11} & D_{12} & D_{13} & 0 & 0 \\ B_{21} & B_{22} & B_{23} & D_{21} & D_{22} & D_{23} & 0 & 0 \\ B_{31} & B_{32} & B_{33} & D_{31} & D_{32} & D_{33} & 0 & 0 \\ 0 & 0 & 0 & 0 & 0 & 0 & H_{44} & H_{45} \\ 0 & 0 & 0 & 0 & 0 & 0 & H_{54} & H_{55} \end{bmatrix} \quad (17)$$

$$A_{ij} = \int_{-\frac{h}{2}}^{\frac{h}{2}} Q_{ij}\, dz \rightarrow A_{ij} = \sum_{k=1}^{N_l} \bar{Q}_{ij}^{k}(h_k - h_{k+1}) \qquad i,j = 1,2,6 \quad (18)$$

$$B_{ij} = \frac{1}{2}\int_{-\frac{h}{2}}^{\frac{h}{2}} Q_{ij} z\, dz \rightarrow B_{ij} = \sum_{k=1}^{N_l} \bar{Q}_{ij}^{k} z(h_k^2 - h_{k+1}^2) \qquad i,j = 1,2,6 \quad (19)$$

$$D_{ij} = \frac{1}{3}\int_{-\frac{h}{2}}^{\frac{h}{2}} Q_{ij} z^2\, dz \rightarrow D_{ij} = \sum_{k=1}^{N_l} \bar{Q}_{ij}^{k} z^2(h_k^3 - h_{k+1}^3) \qquad i,j = 1,2,6 \quad (20)$$

$$H_{ij} = K_0 \int_{-\frac{h}{2}}^{\frac{h}{2}} Q_{ij}\, dz \rightarrow H_{ij} = K_0 \sum_{k=1}^{N_l} \bar{Q}_{ij}^{k}(h_k - h_{k+1}) \qquad i,j = 4,5 \quad (21)$$

$$S = S_{sh} + S_{st} \quad (22)$$

4.3. Analysis of Buckling Load by Rayleigh-Ritz Method

The Ritz method involves obtaining the total energy function (Π) by summing the strain energy and the work done by external forces. In order to achieve equilibrium, the total energy function of the structure needs to be minimized. Thus, to minimize the total energy and reach equilibrium, we differentiate the total potential energy with respect to the displacement field coefficients A_{mn}, B_{mn}, and C_{mn}. By setting the resulting differentials equal to zero, we obtain the coefficient matrix [24, 30-31]

$$\Pi = U + V \tag{23}$$

$$\frac{\partial \Pi}{\partial A_{mn}} = \frac{\partial \Pi}{\partial B_{mn}} = \frac{\partial \Pi}{\partial C_{mn}} = 0 \tag{24}$$

$$\begin{bmatrix} L_{11} & L_{12} & L_{13} \\ L_{21} & L_{22} & L_{23} \\ L_{31} & L_{32} & L_{33} \end{bmatrix} \begin{bmatrix} A_{mn} \\ B_{mn} \\ C_{mn} \end{bmatrix} = 0 \tag{25}$$

In order to obtain non-trivial solutions in the equation mentioned earlier, the determinant of the coefficient matrix must equal zero ($|L_{ij}| = 0$). By expanding this equation, we derive the characteristic equation for buckling. Solving this equation allows us to determine the buckling load for different values of m and n. It's important to note that the minimum value of P corresponds to the critical buckling load.

5. Optimization of Grid Shells Using the Multi-Objective Meta-Heuristic Methods

In this section, we focus on addressing the problem of specifying the structure of grid shells composite by transforming it into a multi-objective optimization problem. We then proceed to tackle this problem using multi-objective meta-heuristic approaches. To begin with, we delve into the formulation of multi-objective optimization, where multiple objectives need to be simultaneously considered and optimized. This formulation allows us to effectively handle the complexity and trade-offs involved in the design of grid shells composite structures. Next, we introduce the hybrid multi-objective meta-heuristic method as our chosen approach for solving this problem. This method combines different meta-heuristic techniques to broaden the search space and improve the efficiency of finding optimal solutions. By leveraging the strengths of meta-heuristics, we aim to achieve better performance in optimizing the specified structure of grid shells composite.

5.1. Problem Formulation

Nowadays, the industry requires the construction of composites that can withstand the highest buckling load with the minimum weight possible.

To reduce the weight of our proposed composite grid shell, we should first determine the objective function based on the weight of the structure. Equation (26) presents the weight function, which is the sum of the stiffener's weight and the shell's weight.

$$\begin{aligned} w_{tot} &= w_{st} + w_{sh} \\ &= \rho\left((2n_{st}l_{st}ft) + \left(2m_{st}(2\pi Rft)\right)\right) \\ &+\rho(2\pi RLh) \end{aligned} \tag{26}$$

The other objective function is the buckling load. The buckling load could be obtained from the analytical solution in Section 4.3. It can be determined by solving the equation $|L_{ij}| = 0$ which is the determinant of the coefficient matrix in equation (25). We refer to this problem as MWMB, which stands for Minimum Weight Maximum Buckling Load problem.

The parameters of the objective functions are the couple number of helical stiffeners, the unit cell number in shell height, and also ribs thickness and width. Notably, lower and upper bounds for each variable were defined. In Table 1, variables are presented along with their upper and lower bounds.

Table 1. Variables and their ranges

Variable	Ranges
n_{st} : Couple helical stiffeners number	$2-12$
m_{st} : Unit cell number in height shell	$2-12$
$f(mm)$: Rib width	$2-12$
$t(mm)$: Rib thickness	$2-12$

5.2. Multi-Objective Meta-Heuristic Methods

In [3], the authors presented an extension of the popular and efficient Particle Swarm Optimization (PSO) algorithm to handle multiobjective optimization problems. This extension, known as MOPSO, integrates the concept of Pareto dominance into PSO. MOPSO introduces a leader particle that guides other particles in the swarm, maintains a historical record of dominated solutions in an external repository, and optionally incorporates a mutation operator. These modifications allow MOPSO to effectively explore and find a diverse set of solutions that achieve trade-offs between multiple objectives.

In [2], the authors introduced the NSGAII algorithm as an efficient solution for multiobjective optimization problems. This algorithm has gained popularity in the scientific literature because of its useful features such as elitism, fast nondominated sorting, and the crowding distance operator. These features contribute to the algorithm's ability to maintain a diverse set of solutions that cover a wide range of trade-offs between different objectives.

To tackle complex problems with challenging search spaces, hybrid multi-objective optimization methods have emerged. These methods combine the desirable features of different algorithms in order to find optimal solutions. Hybrid multiobjective optimization methods have been gaining popularity, and a general framework for combining evolutionary multiobjective optimization algorithms was proposed in [32].

In this research, we combine two stochastic multi-objective optimization algorithms, NSGAII and MOPSO, to tackle MWMB. These two algorithms have different search processes. NSGAII utilizes elitism, sorting, and crowding distance calculations to improve the spread of solutions and maintain diversity among the Pareto Optimal solutions.

The crowding comparisons help prevent the algorithm from converging too quickly. On the other hand, MOPSO does not use genetic operators and has a different information-sharing mechanism compared to NSGAII. In MOPSO, a special solution known as a leader is employed to guide the other particles. The particles explore the solution space by adjusting their velocity and inertia weight. However, MOPSO can sometimes get stuck in local optima for complex problems.

The aim of the hybrid model is to enhance the overall search process of the algorithm by combining NSGAII and MOPSO, which utilize different approaches to explore and exploit the search space.

1. Start
2. Initialize the parameters of the optimization problem,
3. Initialize the parameters of NSGAII,
4. Initialize the parameters of MOPSO,
5. Initialize the population and evaluate the objective functions,
6. Perform non-dominating sorting and construct the nondomination levels,
7. Calculate the crowding distance for each nondomination level and rank the population,
8. For each generation:
9. Start NSGAII algorithm
   a) Using the upper half of the population,
   b) Create the offspring based on one-point crossover and mutation,
   c) Evaluate the objective functions for offspring,
   d) Merge population and offspring,
   e) Perform fast nondomination sorting,
   f) Calculate the crowding distance and rank population based on nondomination fronts,
   g) Store the nondominated solutions in list F_1,
10. Start the MOPSO algorithm
    a) Position and cost of particles are initialized based on the lower half of the population,
    b) Store the value of particles as their personal best, pBest,
    c) Determine the domination for the particles,
    d) Initialize the external repository ,
    e) Create a grid and find the grid index,
    f) For each particle
    g) Select the leader for the external repository,
    h) Update the speed and position of the particle,
    i) Determine domination
    j) Update pBest,
11. Add nondominated solutions to the repository,
12. Keep only the nondominated members in the repository,
13. Update grid and grid index,
14. Combine the population of NSGAII and particles of MOPSO,
15. Perform fast nondomination sorting,
16. Calculate the crowding distance for each nondomination level and rank the population,
17. Divide the population into two halves,
18. Increment generation count,
19. Stop the algorithm when it reaches MaxIteration

Fig. 1. The pseudocode of the hybrid method.

One challenge in optimization is the tendency to get stuck in local optima, so the hybrid algorithm seeks a balance between exploration and exploitation to avoid this issue. To prevent premature convergence and achieve a well-distributed Pareto Optimal Front, the population is divided into two halves based on the ranking generated by the nondomination fronts. The better half of the population is further improved using the NSGAII algorithm, while the other half is treated as swarm particles and optimized using MOPSO to ensure their convergence toward the best possible solutions

This algorithm incorporates an exploration phase conducted by the efficient and elitist NSGAII algorithm, which focuses on the best upper half of the population. This exploration process allows the hybrid algorithm to obtain a good understanding of global solutions. On the other hand, the exploitation phase is performed by MOPSO, utilizing the lower half of the population. MOPSO examines the neighborhoods of these lower-ranked particles and adjusts their orientations towards potential global solutions. By doing so, MOPSO aims to improve the overall quality of solutions by exploiting the local search space.

This hybrid algorithm utilizes an efficient approach to explore the search space, enabling it to strike a better balance between exploiting known solutions and exploring new possibilities. By effectively managing the compromise between exploitation and exploration, the algorithm aims to identify the most promising solutions.

NSGAII utilizes an external archive called F1, whereas MOPSO uses a repository to store solutions. At the end of each iteration, the nondominated solution in F1 and the repository are combined and sorted before being stored back in F1. F1 is filled with solutions from different nondominated fronts one at a time until the archive is full. The filling process starts with the first nondominated front of class one, then moves on to the solutions of the second nondominated front, and so on. When F1 reaches its capacity, the algorithm removes any remaining nondominated fronts. During the consideration of the last front, the points with the highest diversity are selected by using a measure called crowding distance values. This selection process helps maintain a diverse and representative set of solutions in F1. The pseudocode of the hybrid method is shown in Figure 1.

As shown in Figure 1, in each generation, the population is divided into two halves. The upper half of the population undergoes exploration using NSGAII, following steps (a)-(g). The offspring are created based on one-point crossover and mutation, and then, evaluate the objective functions for them. Population and offspring are merged and fast nondomination sorting is performed. Then, the crowding distance is calculated, and the population is ranked based on nondomination fronts. Finally, the nondominated solutions are stored in list F_1. The sub-steps (f)-(j) in step 10 are part of an iterative loop that is performed for each particle. Firstly, the leader for the external repository is selected. Next, the speed and position of the particle are updated based on the chosen leader. Subsequently, domination is assessed, and pBest (personal best) is updated accordingly.

5.3. Numerical Results

In this section, we provide the numerical results obtained by applying three multi-objective optimization methods, namely MOPSO, NSGAII, and the hybrid method, to solve MWMB. The population size and number of generations are set to 40 for all methods. The implementation of the code is done in MATLAB, and it is available upon request if needed. All the parameters are given in Table 2.

Table 2. The parameters of NSGAII, MOPSO, and the hybrid method

NSGAII	MOPSO	Hybrid method
nPop=40	nPop=40	nPop=40
MaxIt=40	MaxIt=40	MaxIt=40
PCrossover=0.7	nRep=50	PCrossover=0.7
PMutation=0.4	w=0.5	PMutation=0.4
mr=0.02	c1=1, c2=2	mr=0.02
	alpha=0.1	nRep=50
	beta=2	w=0.5
	gamma=2	c1=1, c2=2
	mu=0.1	alpha=0.1
		beta=2
		gamma=2
		mu=0.1

Figures 2, 3, and 4 present the objective function values of the Pareto front solutions obtained by NSGAII, MOPSO, and the hybrid method, respectively. Additionally, Tables 3, 4, and 5 display the solutions on the Pareto fronts obtained by NSGAII, MOPSO, and the hybrid method, respectively. These Tables provide decision-makers with a range of options to choose from, allowing them to select the solution that aligns most closely with their specific preferences and requirements. Each solution

consists of the values of the couple number of helical stiffeners (n_{st}), the unit cell number in shell height (m_{st}), and also ribs thickness (t) and width (f). The first and second columns of the Tables are the mass (m) and buckling load (b) of the structures corresponding to the solutions.

When comparing various multi-objective optimization methods, the criteria considered are the diversity of solutions found on the Pareto front and their distribution across all regions. Notably, the hybrid method demonstrates greater diversity in its solutions compared to NSGAII. As a result, decision-makers can more easily select the solution that best aligns with their specific preferences and requirements. Figure 4 illustrates that the critical buckling load of solutions obtained by the hybrid method ranges from 0.6 to 1.8 MPa, while the range for NSGAII is from 0.7 to 1.4 MPa, as depicted in Figure 2.

Figure 5 displays the objective function values of the Pareto front solutions obtained by NSGAII at the end of the last iteration of the hybrid method. It can be observed that the range of the critical buckling load of solutions is the same as that of the hybrid method. However, the number of solutions found by NSGAII is lower compared to the hybrid method. This indicates that incorporating MOPSO after NSGAII improves the overall process.

As depicted in Figure 3, MOPSO exhibits superior performance compared to NSGAII in terms of the diversity of solutions found on the Pareto front. This suggests that incorporating MOPSO after NSGAII helps alleviate the weaknesses of NSGAII to solve MWMB.

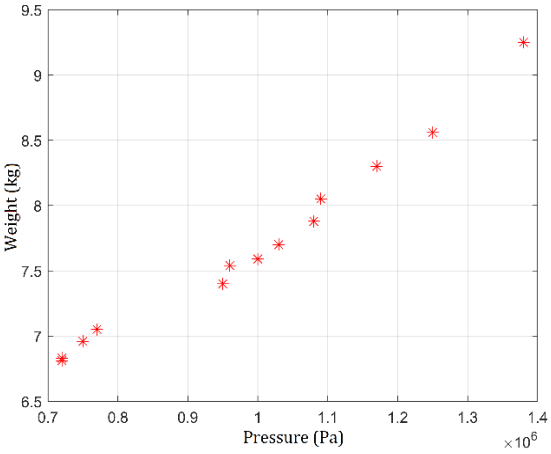

Fig.2. The Pareto front discovered by NSGAII

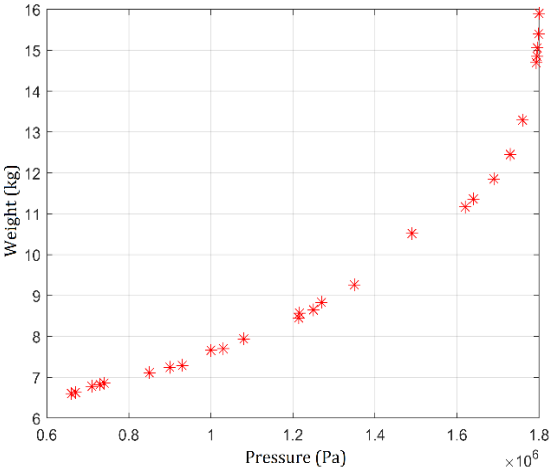

Fig. 3. The Pareto front found by MOPSO

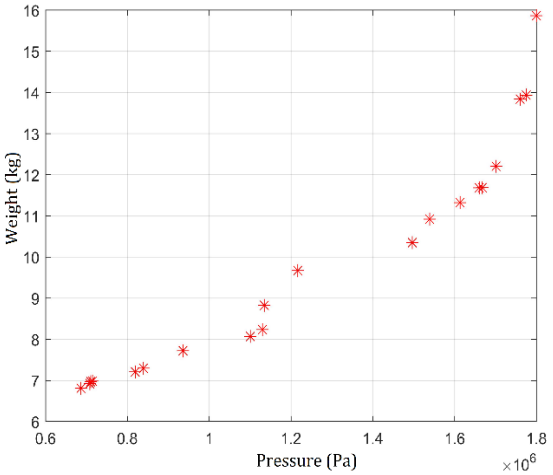

Fig. 4. The Pareto front found by the hybrid Method

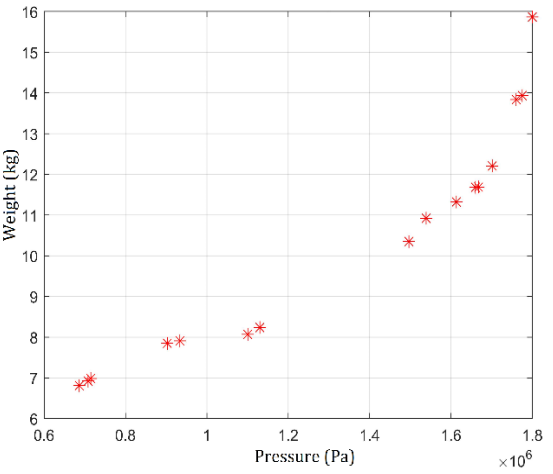

Fig.5. The Pareto front obtained by NSGAII at the completion of the final iteration of the hybrid method.

Table 3. The solutions were obtained on the Pareto front using NSGAII.

Solution Number	$m(kg)$	$b(MPa)$	n_{st}	m_{st}	$t(mm)$	$f(mm)$
1	8.56	1.25	12	5	3	12
2	7.4	0.95	9	3	2	12
3	8.3	1.17	12	4	3	12
4	7.59	1	9	4	2	12
5	6.83	0.72	7	2	2	6
6	7.88	1.08	12	5	2	12
7	8.05	1.09	12	3	3	12
8	9.25	1.38	12	5	4	12
9	7.7	1.03	12	4	2	12
10	6.81	0.72	6	2	2	6
11	6.96	0.75	9	3	2	6
12	7.05	0.77	9	4	2	6
13	7.54	0.96	12	3	2	12

Table 4. The solutions obtained on the Pareto front using MOPSO

Solution Number	$m(kg)$	$b(MPa)$	n_{st}	m_{st}	$t(mm)$	$f(mm)$
1	6.63	0.67	2	2	3	2
2	11.17	1.62	11	5	7	12
3	9.26	1.35	12	12	2	12
4	13.29	1.76	12	8	7	12
5	11.85	1.69	12	9	5	12
6	8.45	1.214	3	2	8	12
7	8.83	1.27	11	10	2	12
8	7.66	1	2	2	5	12
9	7.7	1.03	6	2	4	12
10	15.9	1.8	10	9	9	12
11	11.36	1.64	12	8	5	12
12	14.7	1.793	12	10	7	12
13	14.85	1.795	10	9	8	12
14	7.29	0.93	4	2	3	12
15	8.65	1.25	12	9	2	12
16	7.24	0.9	3	2	3	12
17	6.82	0.73	2	2	2	8
18	7.94	1.08	6	3	4	11
19	10.52	1.49	8	12	3	12
20	8.57	1.216	3	3	6	12
21	6.6	0.66	2	2	2	2
22	12.45	1.73	10	6	8	12
23	15.06	1.796	8	6	12	12
24	7.11	0.85	6	2	2	12
25	6.86	0.74	2	2	2	9
26	6.78	0.71	2	2	2	7
27	15.4	1.799	12	11	7	12

Table 5. The solutions obtained on the Pareto front using the hybrid method

Solution Number	$m(kg)$	$b(MPa)$	n_{st}	m_{st}	$t(mm)$	$f(mm)$
1	8.06	1.1	3	2	7	11
2	12.2	1.7	8	4	11	12
3	7.21	0.82	6	2	4	7
4	6.98	0.715	5	4	6	2
5	8.83	1.14	2	4	7	9
6	6.92	0.708	8	5	4	2
7	9.67	1.21	10	12	4	7
8	10.35	1.46	7	5	11	7
9	10.9	1.55	6	6	7	11
10	7.3	0.84	9	3	3	7
11	13.93	1.78	10	6	10	12
12	11.69	1.667	8	4	10	12
13	6.81	0.69	6	8	2	2
14	15.86	1.805	9	8	11	11
15	8.23	1.13	5	4	4	11
16	11.68	1.660	5	4	11	12
17	11.32	1.62	6	6	7	12
18	13.84	1.77	9	6	11	11
19	6.97	0.71	4	4	6	2
20	7.72	0.93	8	4	4	7

6. Conclusions

This study focuses on the buckling behavior of grid-stiffened composite shells under external hydrostatic pressure. It utilizes the first-order shear deformation theory (FSDT) and the Ritz method to calculate the critical buckling load. Factors such as shell thickness, angle of helical stiffeners, rib section area, and the number of stiffeners are analyzed to determine their impact on the buckling load. The study applies three multi-objective optimization algorithms to find the parameter values that minimize the structure's mass and maximize the critical buckling load.

The algorithms used are Nondominated Sorting Genetic Algorithm II (NSGAII), Multiobjective Particle Swarm Optimization (MOPSO), and a hybrid method combining NSGAII and MOPSO. The hybrid method divides the population into two groups and utilizes NSGAII and MOPSO to explore and exploit the solution space effectively. The obtained Pareto optimal front provides various solutions across different regions, giving decision-makers the flexibility to choose the solution that best aligns with their preferences. The solutions obtained by the different algorithms are compared based on their diversity and spread across the Pareto front.

As a future study, we aim to develop a mathematical function that incorporates the critical buckling pressure and weight to visualize all solutions on the Pareto front. This visualization will assist decision-makers in easily selecting the solution that best suits their specific preferences and requirements.

Nomenclature

z	Distance from the middle surface;
$\varepsilon_{ij}^{(0)}$	Middle surface normal strains;
$\gamma_{ij}^{(0)}$	Middle surface shear strains;
k_{ij}	Surface curvatures;
A_{st}	Cross-section area of stiffeners;
E_l	Longitudinal modulus of stiffeners;

c $Cos\ \varphi$;

s $Sin\ \varphi$;

F_{lz} Force applied to the stiffeners;

N_{ij} Resultant stress;

M_{ij} Resultant momentums;

Q_{ij} Stiffness coefficients;

h_k The kth layer;

h_{k+1} The (k+1)th layer;

S_{sh} Equivalent stiffness matrix for shell;

S_{st} Equivalent stiffness matrix for stiffeners;

U Strain energy;

V Potential energy;

M_i Moments applied to unit cell;

G_{ij} Shear modulus;

a Length of unit cell;

b Width of unit cell;

A_{ij}^{st} Extensional stiffness of stiffeners;

B_{ij}^{st} Coupling stiffness of stiffeners;

L_{ij} Coefficient matrix;

H_{ij}^{st} Shear stiffness of stiffeners;

$\bar{Q}_{ij}^{k}$ Reduced stiffness coefficients;

D_{ij}^{st} Bending stiffness of stiffeners;

Conflicts of Interest

The author declares that there is no conflict of interest regarding the publication of this manuscript. In addition, the authors have entirely observed the ethical issues, including plagiarism, informed consent, misconduct, data fabrication and/or falsification, double publication and/or submission, and redundancy.

References

[1] Coello, C.A.C., Pulido, G.T. and Lechuga, M.S., 2004. Handling multiple objectives with particle swarm optimization. IEEE Transactions on evolutionary computation, 8(3), pp.256-279.

[2] Coello, C.C. and Lechuga, M.S., 2002, May. MOPSO: A proposal for multiple objective particle swarm optimization. In Proceedings of the 2002 Congress on Evolutionary Computation. CEC'02 (Cat. No. 02TH8600) (Vol. 2, pp. 1051-1056). IEEE.

[3] Deb, K., Pratap, A., Agarwal, S. and Meyarivan, T.A.M.T., 2002. A fast and elitist multiobjective genetic algorithm: NSGA-II. IEEE transactions on evolutionary computation, 6(2), pp.182-197.

[4] Sundaram, A., 2020. Combined heat and power economic emission dispatch using hybrid NSGA II-MOPSO algorithm incorporating an effective constraint handling mechanism. IEEE Access, 8, pp.13748-13768.

[5] Kim, C. G., Kang J.-H., 2005, Minimum-weight design of compressively loaded composite plates and stiffened panels for postbuckling strength by genetic algorithm, *Composite structures, 69* (2), pp.239-246.

[6] Kim, D. H., Choi D. H., and Kim, H. S., 2014, Design optimization of a carbon fiber reinforced composite automotive lower arm, *Composites Part B: Engineering, 58*, pp.400-407.

[7] Herath, M.T., Natarajan, S., Prusty, B.G., and John, N. St, 2014, Smoothed finite element and genetic algorithm based optimization for shape adaptive composite marine propellers, *Composite Structures, 109*, pp.189-197.

[8] Sekulski, Z., 2010, Multi-objective topology and size optimization of high-speed vehicle-passenger catamaran structure by genetic algorithm, *Marine Structures, 23*(4), pp.405-433.

[9] Kim, T.D., 2000, Fabrication and testing of thin composite isogrid stiffened panel, *Composite Structures, 49*, pp.21-25.

[10] Ambur, D. R., N. Jaunky, 2001, Optimal design of grid-stiffened panels and shells with variable curvature, *Composite Structures, 52*, pp.173-180.

[11] Zhang, Y.H., X.M. Qiu, D.N. Fang, 2008, Mechanical properties of two novel planar lattice structure, *Solid and Structures, 45*, pp.3751-768.

[12] Yazdani, M., Rahimi, G.H., 2010, The Effects of Helical Ribs' Number and Grid Types on the Buckling of Thin-Walled GFRP Stiffened Shells under Axial Loading, *Journal of Reinforced Plastics and composite, 29*, pp.2568-2575.

[13] Jingxuan, H., Mingfa, R., Qizhong, H., Shanshan, S., & Haoran, C. (2011). Buckling behavior of compression-loaded advanced grid stiffened composite cylindrical shells with reinforced cutouts, *Polymers and Polymer Composites, 19*(4-5), 357-362.

[14] Vasiliev, V.V., Barynin, V.A., Razin, A.F., 2012, Anisogrid composite lattice structures– Development and aerospace applications, *Composite Structures, 94*, pp.1117–1127.

[15] Weber, J.M., Meddendorf, P., 2014, Semi-analytical skin buckling of curved orthotropic grid-stiffened shells", *Composite Structures, 108*, pp.616–624.

[16] Liu, Q., & Paavola, J., 2016, General analytical sensitivity analysis of composite laminated plates and shells for classical and first-order shear deformation theories, *Composite Structures, 127*, pp.88-101.

[17] Deveci, H. Arda, Levent Aydin, and H. Seçil Artem, 2016, Buckling optimization of composite laminates using a hybrid algorithm under Puck failure criterion constraint*, Journal of Reinforced Plastics and Composites, 35* (16), pp.1233-1247.

[18] Ghasemi, A., Hajmohammad, M., 2017, Multi-objective optimization of laminated composite shells for minimum mass/cost and maximum buckling pressure with failure criteria under external hydrostatic pressure. *Struct Multidisc Optim 55*, pp.1051–1062.

[19] Hajmohammad, M., Tabatabaeian, A., Ghasemi, A., and Taheri-Behrooz, F., 2020, A novel detailed analytical approach for determining the optimal design of FRP pressure vessels subjected to hydrostatic loading: Analytical model with experimental validation, *Composites Part B: Engineering 183*, 107732.

[20] Ghasemi, A., Tabatabaeian, A., Hajmohammad, M., and Tornabene, F., 2021, Multi-step buckling optimization analysis of stiffened and unstiffened polymer matrix composite shells: A new experimentally validated method, *Composite Structures, 273*, 114280.

[21] Soltani, M., Abolghasemian, R., Shafieirad, M., Abbasi, Z., Amiri Mehra, AH., and Ghasemi, A., 2022, Multi-objective optimization of lateral stability strength of transversely loaded laminated composite beams with varying I-section*, Journal of Composite Materials 56*(12), pp.1921-1939.

[22] Hosseni, H.S., Khourshidi, K. and Payandeh, H., 2009. Vibration analysis of moderately thick rectangular plates with internal line support using the Rayleigh-Ritz approach.

[23] Arshid, E., Amir, S. and Loghman, A., 2021. Thermal buckling analysis of FG graphene nanoplatelets reinforced porous nanocomposite MCST-based annular/circular microplates. Aerospace Science and Technology, 111, p.106561.

[24] Soheil Shamaee, M. and Ghasemi, A.R., 2023. Minimal Mass and Maximal Buckling Load of Composite Hexagonal-Triangle Grid Structure using FSDT under External Hydrostatic Pressure. Mechanics Of Advanced Composite Structures, 10(2), pp.309-318.

[25] Reddy, J.N., 2004, *Mechanic of Laminated Composite Plates and Shells: Theory and Analysis* (Second Edition), CRC PRESS.

[26] Jaunky, N., N.F. Knight Jr, and D.R. Ambur, 1996, Formulation of an improved smeared stiffener theory for buckling analysis of grid-

stiffened composite panels, *Composites Part B: Engineering, 27* (5), pp.519-526.

[27] Kidane, S., Li, G., Helms J., Pang S. S., and Woldesenbet E., 2003, Buckling load analysis of grid stiffened composite cylinders, *Composites Part B: Engineering, 34* (1), pp.1-9.

[28] Sadeghifar, M., Bagheri, M., and Jafari, A. A., 2011, Buckling analysis of stringer-stiffened laminated cylindrical shells with nonuniform eccentricity, *Archive of Applied Mechanics, 81*, pp.875-886.

[29] Shakib, M., 2007, Mechanics of Composite Structures (1), University of Imam Hussein press.

[30] Ghasemi, A.R. and Hajmohammad, M.H., 2015. Minimum-weight design of stiffened shell under hydrostatic pressure by genetic algorithm. Steel and Composite Structures, 19(1), pp.75-92.

[31] Ghasemi, A.R. and Hajmohammad, M.H., 2018. Mass and buckling criterion optimization of stiffened carbon/epoxy composite cylinder under external hydrostatic pressure. Latin American Journal of Solids and Structures, 15.

[32] Sindhya, K., Miettinen, K. and Deb, K., 2012. A hybrid framework for evolutionary multi-objective optimization. IEEE Transactions on Evolutionary Computation, 17(4), pp.495-511.